



Elastodynamic Marchenko focusing, Green's function retrieval and imaging

Kees Wapenaar and Evert Slob

summary

Building on acoustic autofocusing in 1D media, we previously proposed acoustic Marchenko imaging for 1D and 3D media. Recently, the first steps have been set towards extending the single-sided Marchenko method to the elastodynamic situation. Here we discuss the extension of single-sided Marchenko focusing, Green's function retrieval and imaging to the elastodynamic situation. With numerical examples in a horizontally layered medium we show that, at least in principle, a true amplitude image can be obtained, free of artefacts related to multiple reflections and wave conversions. The method can be extended to 3D situations, in a similar way as we extended the acoustic 1D method to the 3D situation.



Introduction

Building on work of Rose (2002) and Brogini and Snieder (2012) on acoustic autofocusing in 1D media, we proposed acoustic Marchenko imaging for 1D and 3D media (Slob et al., 2014; Wapenaar et al., 2014). Marchenko imaging can be summarised as follows. Given the reflection response at the surface (after surface-related multiple elimination) and an estimate of the direct arrival of the Green's function between a virtual-source point in the subsurface and a receiver at the surface, an iterative solution of the 3D single-sided Marchenko equation gives the complete Green's functions (including the correct internal multiples) between the virtual source in the subsurface and receivers at the surface. Subsequently, these Green's functions are used to redatum the reflection response from the surface to the depth of the virtual sources in the subsurface. This redatumed reflection response, which is free of disturbances by the overburden (including the internal multiples), is subsequently used for imaging.

Recently, Wapenaar and Slob (2014) and da Costa et al. (2014) made the first steps towards extending the single-sided Marchenko method to the elastodynamic situation. Here we review the single-sided elastodynamic Green's function representations (Wapenaar, 2014) and discuss some aspects of elastodynamic Marchenko focusing. Next we discuss how to use the retrieved elastodynamic Green's functions for redatuming and imaging.

Single-sided Green's function representations

For simplicity we consider horizontally layered media, so that all our expressions can be given in the (p, τ) -domain, where p is the ray parameter and τ the intercept time. Note, however, that our expressions can also be formulated in the space-time domain for 3D inhomogeneous media (Wapenaar and Slob, 2014). Consider the following elastodynamic Marchenko-type Green's function representations

$$\mathbf{G}^{-,+}(p, z_0, z_i, \tau) + \mathbf{F}_1^-(p, z_0, z_i, \tau) = \int_{-\infty}^{\tau} \mathbf{R}(p, z_0, \tau - \tau') \mathbf{F}_1^+(p, z_0, z_i, \tau') d\tau', \quad (1)$$

$$-\mathbf{G}^{-,-}(p, z_0, z_i, \tau) - \mathbf{F}_1^+(-p, z_0, z_i, -\tau) = -\int_{-\infty}^{\tau} \mathbf{R}(p, z_0, \tau - \tau') \mathbf{F}_1^-(-p, z_0, z_i, -\tau') d\tau'. \quad (2)$$

The boldface symbols are 2×2 matrices, hence

$$\mathbf{R}(p, z_0, \tau) = \begin{pmatrix} R_{P,P} & R_{P,S} \\ R_{S,P} & R_{S,S} \end{pmatrix} (p, z_0, \tau), \quad (3)$$

etc. Here, for example, $R_{P,S}(p, z_0, \tau)$ is the plane-wave reflection response at the acquisition level z_0 in terms of upgoing P -waves in response to downgoing S -waves. $\mathbf{G}^{-,+}(p, z_0, z_i, \tau)$ and $\mathbf{G}^{-,-}(p, z_0, z_i, \tau)$ are Green's functions, i.e., responses to a virtual source at depth level z_i , observed at z_0 . Here the second superscript refers to the radiation direction of the virtual source at z_i (+ for downward and - for upward radiation), whereas the first superscript (-) denotes that the observed field at z_0 is upward propagating. The elements are organized similar as in equation (3). For example, $G_{P,S}^{-,+}(p, z_0, z_i, \tau)$ represents an upgoing P -wave observed at z_0 , in response to a virtual source for downgoing S -waves at z_i . \mathbf{F}_1^+ and \mathbf{F}_1^- are focusing functions in a reference medium, which is identical to the real medium above the focus level z_i and homogeneous below this level. $\mathbf{F}_1^+(p, z_0, z_i, \tau)$ is defined such that, when emitted from z_0 into the medium, it focuses at $\tau = 0$ at z_i . The superscript + denotes that it propagates downward (i.e., in the positive z -direction) at z_0 . Its elements are organized in a similar way as in equation (3). Hence, the elements in the left column, $F_{P,P}^+(p, z_0, z_i, \tau)$ and $F_{S,P}^+(p, z_0, z_i, \tau)$, represent the downward propagating P - and S -waves at z_0 , respectively, which give rise to a P -wave focus at z_i . Similarly, the elements in the right column cause an S -wave focus at z_i . $\mathbf{F}_1^-(p, z_0, z_i, \tau)$ is the upward (-) reflected part of the focusing function at z_0 (see Wapenaar et al. (2014) for a more detailed discussion).

Representations (1) and (2) provide the basis for retrieving the Green's functions $\mathbf{G}^{-,+}$ and $\mathbf{G}^{-,-}$. The reflection response $\mathbf{R}(p, z_0, \tau)$ in these representations is obtained from measurements at the top boundary z_0 only. Once the focusing functions \mathbf{F}_1^+ and \mathbf{F}_1^- at z_0 are known, the Green's functions follow from equations (1) and (2).



----- $z_0 = 0\text{m}$	
$c_P = 2000\text{ m/s}$	$c_S = 1000\text{ m/s}$
----- $z = 400\text{m}$	
$c_P = 4500\text{ m/s}$	$c_S = 3500\text{ m/s}$
----- $z = 800\text{m}$	
----- $z_i = 1000\text{m}$	
$c_P = 2500\text{ m/s}$	$c_S = 1500\text{ m/s}$
----- $z = 1400\text{m}$	
$c_P = 4000\text{ m/s}$	$c_S = 2500\text{ m/s}$

Figure 1 Horizontally layered model.

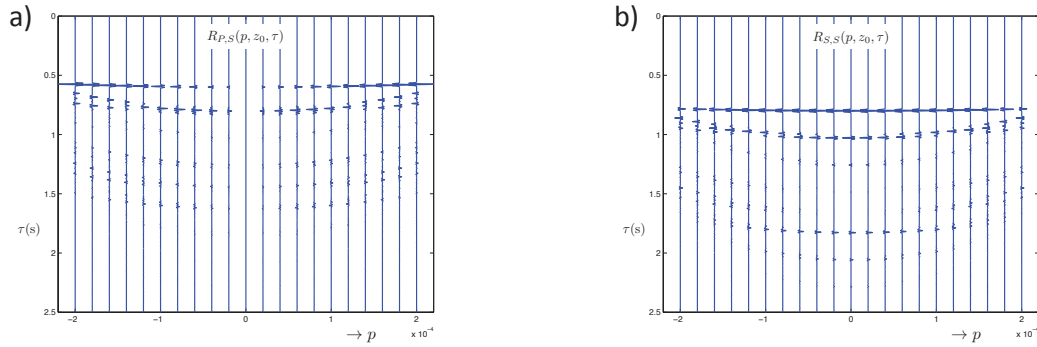


Figure 2 Reflection responses $R_{P,S}(p, z_0, \tau)$ and $R_{S,S}(p, z_0, \tau)$ for a range of rayparameters.

Single-sided Marchenko focusing and Green's function retrieval

Under certain conditions (Wapenaar, 2014), the focusing functions \mathbf{F}_1^+ and \mathbf{F}_1^- can be obtained from the single-sided reflection response \mathbf{R} by solving equations (1) and (2) via an iterative Marchenko scheme in the time intervals where $\mathbf{G}^{-,+}$ and $\mathbf{G}^{-,-}$ are zero. This assumes not too complex media, so that the overlap in time of the functions on the left-hand sides in equations (1) and (2) is minimum. The scheme is initiated with the inverse of the direct and forward scattered parts of the transmission response of the medium between z_0 and z_i . Hence, this requires an estimate of the medium between these two depth levels. It is expected that the requirements for a model which explains forward scattering are less severe than the requirements for a model which explains backward scattered multiple reflections.

We illustrate the method for the horizontally layered model of Figure 1, in which $z_0 = 0\text{m}$ and $z_i = 1000\text{m}$. Figure 2 shows two components of the reflection response at the surface, $\mathbf{R}(p, z_0, \tau)$, for a range of p -values. In the following we choose a fixed p -value of $p = .0002\text{s/m}$ (i.e., the right-most trace in both figures). The $\tau < 0$ part of the top trace in Figure 3a shows the focusing function $\mathbf{F}_1^+(p, z_0, z_i, \tau)$ obtained from $\mathbf{R}(p, z_0, \tau)$ after four iterations of the Marchenko scheme. As a matter of fact, it shows the superposition of the elements $F_{P,S}^+(p, z_0, z_i, \tau)$ and $F_{S,S}^+(p, z_0, z_i, \tau)$ in the right column of \mathbf{F}_1^+ , i.e., the downward propagating P - and S -waves at $z_0 = 0$, which give rise to an S -wave focus at z_i . The other traces in this figure show how this complex wave field propagates through the medium and causes a well-defined S -wave focus at $\tau = 0$ and $z_i = 1000\text{m}$. The focal point acts as a virtual source for downgoing S waves, which, after propagation and scattering, reach the top surface z_0 in the form of upgoing P and S -waves (the right column of $\mathbf{G}^{-,+}$ in equation (1)). A similar experiment, with the left column of \mathbf{F}_1^+ emitted from z_0 into the medium, yields a P -wave focus at z_i , which acts as a virtual source for downgoing P -waves, finally causing upgoing P - and S -waves at the top surface z_0 (the left column of $\mathbf{G}^{-,+}$ in equation (1)). This is not shown because of space constraints.

Note that the result in Figure 3a lacks a virtual source for upgoing S -waves. Equation (2) suggests to emit the time-reversal of $-\mathbf{F}_1^-$ (for opposite rayparameter) from z_0 into the medium, which gives $-\mathbf{G}^{-,-}(p, z_0, z_i, \tau)$, i.e., the response at z_0 to a virtual source for upgoing waves at z_i . We combine the responses to \mathbf{F}_1^+ (Figure 3a) and the time-reversal of $-\mathbf{F}_1^-$. The superposition of the illuminating wave fields at z_0 reads (in simplified notation) $\mathbf{F}_1^+(p, \tau) - \mathbf{F}_1^-(-p, -\tau)$. The superposition of their responses at z_0 (i.e., the sum of the left-hand sides of equations (1) and (2)) gives $\mathbf{G}^{-,+}(p, \tau) + \mathbf{F}_1^-(p, \tau) -$

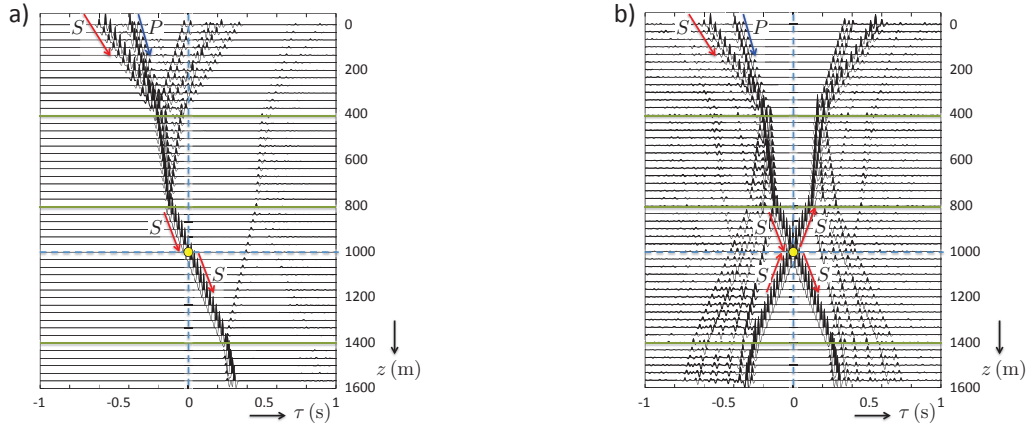


Figure 3 Single-sided Marchenko focusing. (a) Illumination from above by $\mathbf{F}_1^+(p, \tau)$. (b) Illumination from above by $\mathbf{F}_1^+(p, \tau) - \mathbf{F}_1^+(-p, -\tau)$, combined with its time-reversal.

$\mathbf{G}^{-,-}(p, \tau) - \mathbf{F}_1^+(-p, -\tau)$. Hence, the total field at z_0 is given by $\mathbf{H}(p, \tau) = \mathbf{F}_1^+(p, \tau) + \mathbf{F}_1^+(-p, -\tau) + \mathbf{G}^{-,+}(p, \tau) - \mathbf{F}_1^+(-p, -\tau) - \mathbf{F}_1^+(-p, -\tau) - \mathbf{G}^{-,-}(p, \tau)$. Analogous to the procedure proposed by Brogini and Snieder (2012) for the scalar case, we combine $\mathbf{H}(p, \tau)$ with its time-reversal (for opposite ray-parameter), according to $\mathbf{H}(p, \tau) + \mathbf{H}(-p, -\tau) = \mathbf{G}(p, \tau) + \mathbf{G}(-p, -\tau)$, with $\mathbf{G}(p, \tau) = \mathbf{G}^{-,+}(p, z_0, z_i, \tau) - \mathbf{G}^{-,-}(p, z_0, z_i, \tau)$. Hence, with this operation the focusing functions are cancelled, leaving the Green's function and its time-reversal. Applying this operation at all depth levels yields Figure 3b. Note that the $\tau > 0$ part clearly shows the response to a virtual source at z_i , radiating downgoing and upgoing S -waves into the medium. Applying the same process with the left columns of all matrices yields a virtual source at z_i for downgoing and upgoing P -waves (not shown). Note that for the generation of Figure 3, a model of the true medium has been used, but this was done only to visualize the propagation of the waves through the medium. The Green's functions $\mathbf{G}^{-,+}(p, z_0, z_i, \tau)$ and $\mathbf{G}^{-,-}(p, z_0, z_i, \tau)$ are covered by the upper traces only.

Elastodynamic Marchenko imaging

The reciprocals of the retrieved Green's functions, i.e., $\mathbf{G}^{+,+}(p, z_i, z_0, \tau) = -\{\mathbf{G}^{-,-}(-p, z_0, z_i, \tau)\}^t$ and $\mathbf{G}^{-,+}(p, z_i, z_0, \tau) = \{\mathbf{G}^{-,+}(-p, z_0, z_i, \tau)\}^t$ (where superscript t denotes transposition) are mutually related via the reflection response at z_i , according to

$$\mathbf{G}^{-,+}(p, z_i, z_0, \tau) = \int_{-\infty}^{\tau} \mathbf{R}(p, z_i, \tau - \tau') \mathbf{G}^{+,+}(p, z_i, z_0, \tau') d\tau' \quad (4)$$

(Riley and Claerbout, 1976; Wapenaar et al., 2000; Amundsen, 2001). This expression states that the downgoing field $\mathbf{G}^{+,+}$ at z_i , convolved with the reflection response \mathbf{R} at z_i , gives the upgoing field $\mathbf{G}^{-,+}$ at z_i . Note that $\mathbf{G}^{+,+}$ and $\mathbf{G}^{-,+}$ are defined in the actual medium, whereas $\mathbf{R}(p, z_i, \tau)$ is defined in a reference medium that is identical to the actual medium below z_i and reflection-free above z_i . Resolving \mathbf{R} from equation (4) involves "seismic interferometry by deconvolution" (Snieder et al., 2006; Vasconcelos and Snieder, 2008; van der Neut et al., 2011). We illustrate this with a numerical example. Figure 2 shows the elements of the reflection response $\mathbf{R}(p, z_0, \tau)$ at the surface, for a range of p -values. Similar as above, the Green's functions are retrieved via the Marchenko scheme, but this time for all p -values. Next, the reflection response at z_i , $\mathbf{R}(p, z_i, \tau)$, is resolved from these Green's functions by inverting equation (4) for each p -value. This "redatumed" reflection response is shown in Figure 4. Despite the complexity of the reflection response in Figure 2, Figure 4 clearly shows the response of the single reflector below z_i (the interface at $z = 1400$ m, see Figure 1). The p -dependent reflection coefficients are retrieved from these reflection responses after envelope detection. They are denoted by the blue marks in Figure 5. The green curves in this figure are the modeled p -dependent reflection coefficients of the interface at $z = 1400$ m. Note that for this idealized example the match is perfect. Repeating this procedure for all depth levels z_i yields an image in the (p, z) domain (not shown).

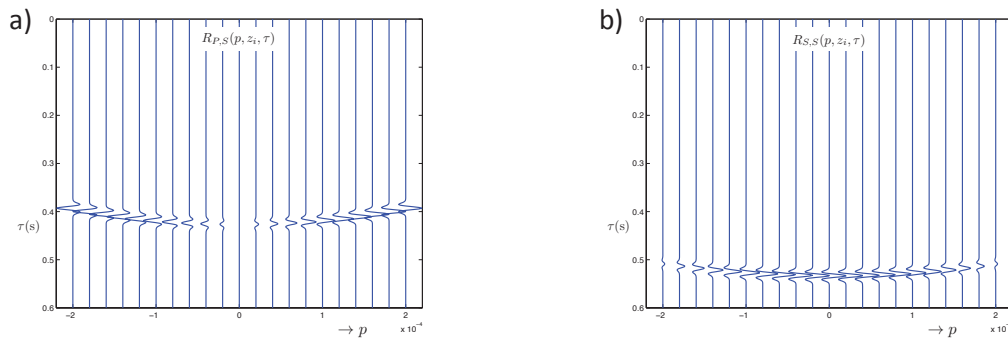


Figure 4 Redatumed reflection responses $R_{P,S}(p, z_i, \tau)$ and $R_{S,S}(p, z_i, \tau)$.

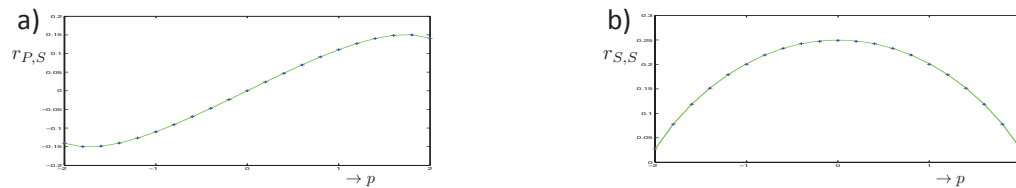


Figure 5 Local reflection coefficients $r_{P,S}(p)$ and $r_{S,S}(p)$ obtained from Figure 4 (blue marks), compared with the p -dependent reflection coefficients of the interface at $z = 1400$ m (green curves).

Conclusions

We have discussed an extension of single-sided Marchenko focusing, Green's function retrieval and imaging to elastic media. With numerical examples in a horizontally layered medium we have shown that, at least in principle, a true amplitude image can be obtained, free of artefacts related to multiple reflections and wave conversions. The method can be extended to 3D situations, in a similar way as we extended the acoustic 1D method to 3D. The representations for this 3D extension have been formulated (Wapenaar, 2014; da Costa et al., 2014). An important research question concerns the requirements with respect to the initial estimate of the Green's functions, which in principle should contain the direct and forward scattered transmission response. Sampling issues also require further research.

References

- Amundsen, L. [2001] Elimination of free-surface related multiples without need of the source wavelet. *Geophysics*, **66**(1), 327–341.
- Broggini, F. and Snieder, R. [2012] Connection of scattering principles: a visual and mathematical tour. *Eur. J. Phys.*, **33**, 593–613.
- da Costa, C.A., Ravasi, M., Curtis, A. and Meles, G.A. [2014] Elastodynamic Green's function retrieval through single-sided Marchenko inverse scattering. *Phys. Rev. E*, **90**, 063201.
- Riley, D.C. and Claerbout, J.F. [1976] 2-D multiple reflections. *Geophysics*, **41**, 592–620.
- Rose, J.H. [2002] 'Single-sided' autofocusing of sound in layered materials. *Inverse Probl.*, **18**, 1923–1934.
- Slob, E., Wapenaar, K., Broggin, F. and Snieder, R. [2014] Seismic reflector imaging using internal multiples with Marchenko-type equations. *Geophysics*, **79**(2), S63–S76.
- Snieder, R., Sheiman, J. and Calvert, R. [2006] Equivalence of the virtual-source method and wave-field deconvolution in seismic interferometry. *Phys. Rev. E*, **73**, 066620.
- van der Neut, J., Thorbecke, J., Mehta, K., Slob, E. and Wapenaar, K. [2011] Controlled-source interferometric redatuming by crosscorrelation and multidimensional deconvolution in elastic media. *Geophysics*, **76**(4), SA63–SA76.
- Vasconcelos, I. and Snieder, R. [2008] Interferometry by deconvolution: Part 2 - Theory for elastic waves and application to drill-bit seismic imaging. *Geophysics*, **73**(3), S129–S141.
- Wapenaar, K. [2014] Single-sided Marchenko focusing of compressional and shear waves. *Phys. Rev. E*, **90**, 063202.
- Wapenaar, K., Fokkema, J., Dillen, M. and Scherpenhuijsen, P. [2000] One-way acoustic reciprocity and its applications in multiple elimination and time-lapse seismics. *SEG, Expanded Abstracts*, 2377–2380.
- Wapenaar, K. and Slob, E. [2014] On the Marchenko equation for multicomponent single-sided reflection data. *Geophys. J. Int.*, **199**, 1367–1371.
- Wapenaar, K., Thorbecke, J., van der Neut, J., Broggin, F., Slob, E. and Snieder, R. [2014] Marchenko imaging. *Geophysics*, **79**(3), WA39–WA57.